Received: 22 July 2019 | Revised: 29 February 2020 | Accepted: 13 April 2020

DOI: 10.4218/etrij.2019-0358

ORIGINAL ARTICLE

ETRI Journal WILEY

Improving PAPR performance of filtered OFDM for 5G communications using PTS

Yasir Amer Al-Jawhar[1,2] | Khairun N. Ramli[1] | Montadar Abas Taher[3] | Nor Shahida M. Shah[4] | Salama A. Mostafa[5] | Bashar Ahmed Khalaf[5]

[1]Faculty of Electrical and Electronic Engineering, Universiti Tun Hussein Onn Malaysia, Batu Pahat, Johor, Malaysia

[2]Iraqi Ministry of Communications, Baghdad, Iraq

[3]Department of Communications Engineering, College of Engineering, University of Diyala, Diyala, Iraq

[4]Faculty of Engineering Technology, Universiti Tun Hussein Onn Malaysia, Pagoh, Mure, Johor, Malaysia

[5]Faculty of Science Computer and Information Technology, Universiti Tun Hussein Onn Malaysia, Batu Pahat, Johor, Malaysia

Correspondence
Yasir Amer Al-Jawhar, Faculty of Electrical and Electronic Engineering, Universiti Tun Hussein Onn Malaysia, Parit Raja, Batu Pahat, 86400, Johor, Malaysia.
Emails: yasir.jawhar@ieee.org; free_cccc@yahoo.com; ge160127@siswa.uthm.edu.my

The filtered orthogonal frequency division multiplexing (F-OFDM) system has been recommended as a waveform candidate for fifth-generation (5G) communications. The suppression of out-of-band emission (OOBE) and asynchronous transmission are the distinctive features of the filtering-based waveform frameworks. Meanwhile, the high peak-to-average power ratio (PAPR) is still a challenge for the new waveform candidates. Partial transmit sequence (PTS) is an effective technique for mitigating the trend of high PAPR in multicarrier systems. In this study, the PTS technique is employed to reduce the high PAPR value of an F-OFDM system. Then, this system is compared with the OFDM system. In addition, the other related parameters such as frequency localization, bit error rate (BER), and computational complexity are evaluated and analyzed for both systems with and without PTS. The simulation results indicate that the F-OFDM based on PTS achieves higher levels of PAPR, BER, and OOBE performances compared with OFDM. Moreover, the BER performance of F-OFDM is uninfluenced by the use of the PTS technique.

KEYWORDS

5G, bit error rate, filtered orthogonal frequency division multiplexing, out-of-band emission, partial transmit sequence, peak-to-average power ratio

1 | INTRODUCTION

Recently, fifth-generation (5G) networks have drawn more attention from the industrial and academic researchers because of the rapid growth of the communication market. In 5G, several applications have been introduced to accomplish the new requirements of this market, for example, machine-to-machine (M2M), Internet of things (IoT), and vehicle-to-vehicle (V2V) communications [1]. It requires utilizing new systems in the physical layer (PHY) and the fulfillment of the requirements of the novel applications [2]. Therefore, waveform design is one of the several PHY systems that should be reviewed with regard to the spectral efficiency, relaxed synchronization, low latency, and high reliability.

Orthogonal frequency division multiplexing (OFDM) is the multicarrier waveform that has been extensively exploited in various wireless communication systems such as the LTE-A standard in the fourth-generation (4G) networks [3]. Moreover, the OFDM-related systems such as OFDM with index modulation (OFDM-IM) have been recently used in several applications in communications, such as cognitive radio communications, underwater acoustic communications, and cooperative communications. Here, OFDM-IM improves the system performance and system spectral efficiency [4,5]. Although the OFDM communication system

provides several advantages such as simplicity of implementation, high capacity, and the requirement of only one tap equalizer per sub-channel to recompense the multipath fading (low equalization complexity), OFDM is constrained by a few challenges such as the high peak-to-average power ratio (PAPR), signaling synchronization, and frequency leakage [6,7]. In 4G-LTE, PAPR is considered as the central problem of the OFDM system because of the nonlinear behavior of the high-power amplifiers (HPA) at the transmitter. Furthermore, the high out-of-band emission (OOBE) as a result of the sinusoidal characteristic of the OFDM signals results in increased adjacent channel interference (ACI) and inter-symbol interference (ISI). Thus, 10% of the bandwidth is lost as the guard band to isolate the adjoining channels [8,9]. In addition, the OFDM system requires time signaling to maintain the orthogonality among the subcarriers without inter-carrier interference (ICI) [10]. These limitations make the OFDM system unsuitable for 5G applications. Therefore, filtered-based waveforms have been introduced as a waveform candidate to overcome most of the limitations of the OFDM system and to achieve the requirements of 5G applications.

There are three types of filtering-based waveform candidates: the sub-band filtering waveform, subcarrier filtering waveform, and full-band filtering waveform [11]. In the subcarrier filtering waveform, each subcarrier is adopted by the transmitter and receiver filters, for example, filter bank multicarrier (FBMC) and filtered multi-tone (FMT) [12]. Meanwhile, the sub-band filtering waveform divides the whole band into several sub-bands and applies a filter for each sub-band, for example, universal filtered multicarrier (UFMC) [13,14]. However, the full-band filtering waveform is designed to utilize only one filter over the entire OFDM frequency bandwidth. Therefore, it is called filtered OFDM (F-OFDM) [15]. Thus, all the types of waveform candidates can support the 5G requirements depending on the filter design. Meanwhile, the novel waveform candidates display different performances with regard to the spectral efficiency, PAPR, computational complexity, and incumbent legacy of the OFDM systems.

Filtered orthogonal frequency division multiplexing is considered as a waveform candidate for 5G that can achieve several features such as convenient design, support for orthogonal transmission and PAPR reduction techniques, improved spectral efficiency, convenient integration with multi-antenna transmission techniques similarly as the OFDM system, low computational complexity, suppression of OOBE level, low latency, and support for asynchronous transmission [16–18]. However, the high PAPR value continues to be the main problem of the F-OFDM waveform candidate because this system supports orthogonal transmission. The added filter is the main cause for the increase in the PAPR value of the F-OFDM candidate. This is because the filter causes the power distribution among the samples to be wider than that in the OFDM system, which results in a decrease in the mean power of the signal and thereby degradation in the HPA efficiency at the transmitter [9]. However, the F-OFDM system supports the PAPR reduction techniques. Therefore, partial transmit sequence (PTS) [19], selective mapping (SLM) [20], and the interleaving reduction technique [21] can be used to reduce the high PAPR values of F-OFDM [22].

In the literature, several studies have been performed to significantly improve the OFDM spectral efficiency and thereby satisfy the requirements of 5G applications. Abdoli and others [23] proposed the asynchronous F-OFDMA to remove the side lobe leakage and suppress the synchronous signaling of the OFDM system. Abdoli analyzed the BER performance and power spectral density (PSD) of the design proposed in comparison with those of the UFMC waveform candidate. Abdoli observed that his proposed design is superior to the UFMC candidate with regard to the frequency localization and BER performances. Xi and others [24] discussed an upgraded version of F-OFDM waveform with higher flexibility. It was achieved by splitting the bandwidth into several bands and applying filtering to each band to achieve different types of services. Zhang's study concluded that this F-OFDM is the most potential 5G waveform candidate based on his proposed design. Similarly, Wu and others [25] also presented a trial study of the F-OFDM based on spectrum slicing in the real 5G environment. Wu indicated that the proposed waveform design could achieve a high spectrum efficiency for the asynchronous applications in the anticipated 5G networks. Jian [16] discussed the spectral efficiency performance of F-OFDM in a 5G field test. According to Wang's results, the F-OFDM waveform framework can achieve a 100% improvement in spectral efficiency compared with the LTE-OFDM system.

Recently, Liu and others [11] performed a comparative study of the filtering-based waveform candidates. He discussed the full-band filtering candidate in comparison with other waveform candidates in terms of OOBE leakage with and without HPA, low latency, BER, carrier frequency offset (CFO) robustness, and Doppler diversity. Liu's study investigates and compares the F-OFDM waveform candidate based on several aspects. However, a few significant relevant problems that need to be addressed and highlighted continue to exist, such as the PAPR performance and computational complexity.

In this study, the PTS technique is adopted to mitigate the high PAPR value in the F-OFDM system. In addition, the performances in terms of the bit error rate (BER), power spectral efficiency (PSD), and computational complexity of the F-OFDM are verified and compared with those of the OFDM based on the PTS technique. The remaining sections of this article are organized as follows: Section 2 presents

a discussion on the F-OFDM waveform. Section 3 presents the PAPR problem and a discussion on it. The F-OFDM based on PTS is presented in Section 4. The filter design is discussed in Section 5. Section 6 presents an analysis of the simulation results. Finally, Section 7 concludes with a summary.

2 | FILTERED ORTHOGONAL FREQUENCY DIVISION MULTIPLEXING

Filtered orthogonal frequency division multiplexing is a waveform candidate that utilizes one pair of transmitter and receiver filters over the whole frequency bandwidth. Figure 1 illustrates a simple diagram of the F-OFDM. Here, the transmitted signal is passed to the transmitter filter after the OFDM processing to generate the transmitter F-OFDM signal. However, the F-OFDM receiver signal is initially passed to the receiver filter, which is identical to the filter used at the transmitter (spectrum shaping filter). The filter at the receiver filters out the signal received from the neighboring signals. Hence, the receiver filter rejects the contributions of other signals and ensures that the OFDM signal is passed to the next stage without interference from the neighboring signals. That is, the receiver filter separates the filtered OFDM signal from the other accompanying influences before decoding the OFDM signal. Finally, the other operations are accomplished similarly as in the traditional OFDM system.

The main objective of adding the filter to the transmitter is to restrain the high OOBE level of the OFDM system to support the asynchronous transmission and to decrease the latency [26]. Thereby, the spectral efficiency is enhanced, and this enables the system to achieve the 5G technology requirements. In contrast, the incorporation of the filter imposes additional complexity on the system. Furthermore, the PAPR increases because the added filter causes a wider power distribution among the samples compared with the OFDM system, which results in a reduction in the mean signal power and thereby degradation of the PAPR performance. Therefore, the improvement in the spectral efficiency of the F-OFDM would be at the expense of increased PAPR and computational complexity of the system.

3 | PAPR PROBLEM

In general, in multicarrier systems such as OFDM, the baseband signal is passed to the IFFT unit to modulate the subcarriers by the data symbol. Therefore, the OFDM signal is expressed as [27]:

$$s(n)=\frac{1}{\sqrt{NU}}\sum_{k=0}^{NU-1}S_k e^{j2\pi kn/NU},\quad 0\le n\le NU-1, \tag{1}$$

where n is the discrete sampling index, S_k (after constellation mapping) is the kth subcarrier's complex block data, and N represents the number of subcarriers. U is the oversampling factor of the zero-padding operation, which is multiple times of the Nyquist rate to obtain highly accurate PAPR values [28]. The OFDM signal is generated in the time domain by applying the IFFT operation on the subcarriers simultaneously. The subcarriers are generally independent and have different phases. Occasionally, the phases of the subcarriers are in an identical direction. This may result in a high peak power compared with the signal's average power. Accordingly, the PAPR of the OFDM signal is expressed as the ratio of the maximum peak power $|s(n)|^2$ to the signal's average power $E\left\{|s(n)|^2\right\}$ [28],

$$\text{PAPR}=\frac{\text{Max}|s(n)|^2}{E\left\{|s(n)|^2\right\}}, \tag{2}$$

where $E\{.\}$ symbolizes the signal's mean value. Moreover, the complementary cumulative distribution function (CCDF) is generally utilized to evaluate the probability that the signal PAPR exceeds a specific threshold value (PAPR_0) [29]:

$$\Pr(\text{PAPR}\ge\text{PAPR}_0)=1-(1-e^{-\text{PAPR}_0})^{NU} \tag{3}$$

4 | F-OFDM BASED ON PTS

The high PAPR can be considered as a challenge that the F-OFDM system may encounter. The filter at the transmitter causes an increase in the power distribution among the samples because the filter length exceeds the cyclic prefix (CP) period [23]. This operation results in a decrease in the signal's mean power and causes an increase in the gap between the maximum peak power and F-OFDM signal's mean power.

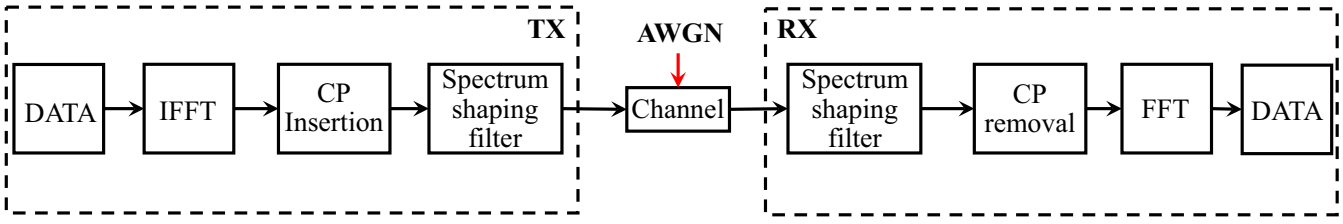

FIGURE 1 F-OFDM block diagram [11]

Therefore, the PAPR of the F-OFDM system is higher than that of the OFDM system.

Partial transmit sequence is an efficient technique employed to decrease an OFDM system's PAPR [30]. PTS depends on the subdivision of the data block into subblocks and the employment of a set of phase rotation factors for weighting these subblocks before recombining them. This technique reduces the PAPR by over 3 dB. However, this is achieved at the cost of an increase in the computational complexity of the system because the PTS technique executes a comprehensive search for all the weighting phases to obtain the optimum phase rotation factor [31]. This is shown in Figure 2.

Figure 2 illustrates the F-OFDM based on the PTS technique (PTS-F-OFDM). Here, a constellation mapping method is used to modulate the input data, such as the quadrature amplitude modulation (QAM) family. Subsequently, the complex baseband signal is converted from serial to parallel. Then, the baseband symbol is subdivided into M subblocks:

$$S(n) = \sum_{m=1}^{M} S_m(n). \tag{4}$$

Thereafter, the zero-padding operation is applied to the subblocks before they are fed to the UN-IFFT units for converting the subblocks from the frequency domain to the time domain. In the time domain, the converted subblocks are multiplied by the set of phase factors and then are recombined to obtain a candidate group. The selection of the phase factor is based on the achievement of the minimum value among the candidates to rotate the joint subblocks. Then, it is considered as side information (SI) to recover the original data. Therefore, the generated OFDM signal that is optimized by the optimum phase rotating factor can be expressed as [32]

$$s(n) = UN - \text{IFFT}\left\{\sum_{m=1}^{M} b_m S_m(n)\right\} = \sum_{m=1}^{M} b_m s_m(n), \tag{5}$$

where

$$b_m = \left\{e^{j2\pi m/R} | m = 0,\ 1,\ \ldots,\ R-1\right\}, \tag{6}$$

where the optimum phase factor is represented by b_m. R denotes the number of elements in the phase rotation factors. Finally, the signal $s(n)$ is passed to the suitably designed spectrum shaping filter for generating the F-OFDM signal, $y(n)$, which is to be sent to the receiver [23]:

$$y(n) = f(n) * s(n), \tag{7}$$

where the finite impulse response (FIR) of the filter coefficients is denoted by $f(n)$. Considering this, the filter is designed with a filter length, L, equal to half of the OFDM symbol length + 1. This filter length is selected to enable the filter to provide better frequency localization and to achieve an effective filtering performance in terms of parameters such as flatness of the passband and sharpness of the transition band. Therefore, a filter length of up to half of the OFDM symbol's length provides the flexibility to design the filter and to ensure ultimate filtering performance so that there is no guard subcarrier between neighboring symbols. Initially, the received signal is manipulated by

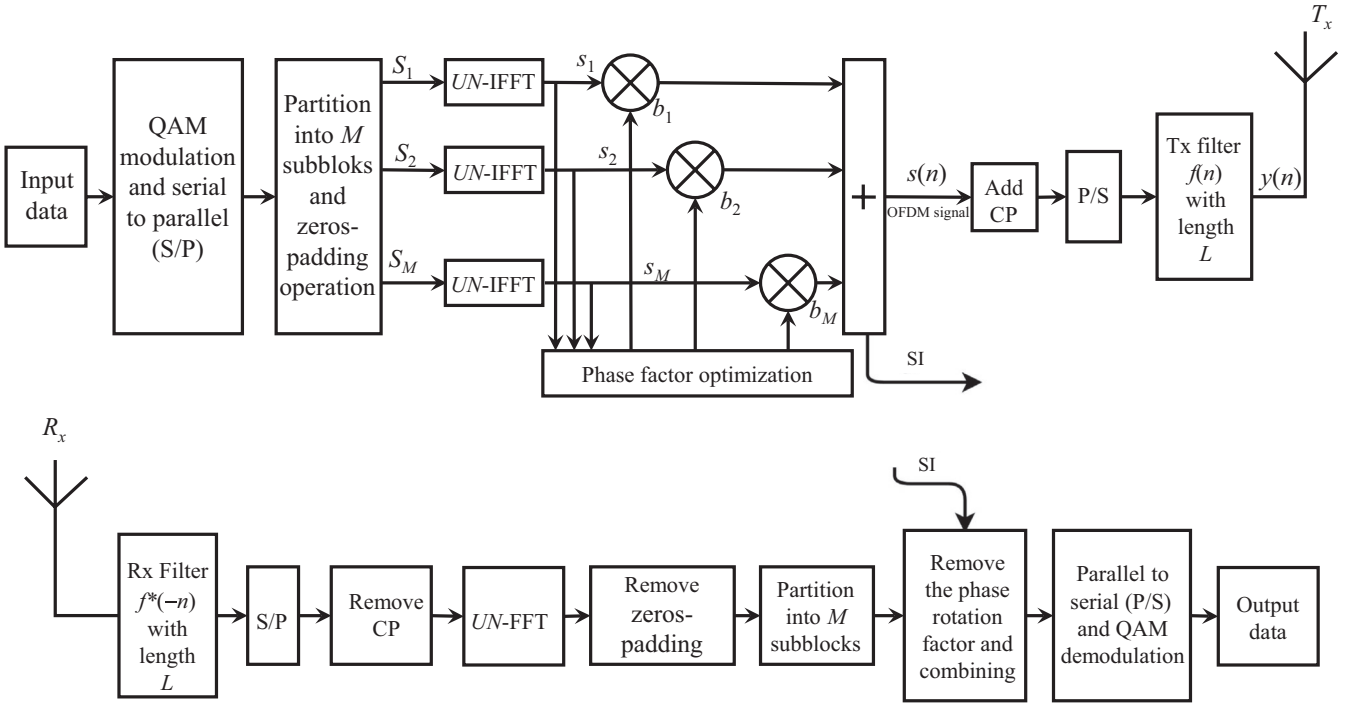

FIGURE 2 PTS-F-OFDM (transmitter and receiver) block diagram

the receiving filter $f^*(-n)$ at the receiver side, which matches the transmitting filter. Therefore, the received signal after passing to the receiving filter is expressed as [10]:

$$d(n) = f(n) * s(n) * f^*(-n). \tag{8}$$

The behavior of the receiving filter causes the isolation of the F-OFDM signal from the contributions of the other adjacent signals, to ensure that the receiver processes performed on the received F-OFDM signal are accomplished without interference with adjacent signals. Hence, the receiver filter (spectrum shaping filter) splits the filtered OFDM signal into the OFDM signal. Moreover, the spectrum shaping filter can be defined as a function of its allocated bandwidth resources, and this definition corresponds to the transmitting F-OFDM. Therefore, it is known for both the transmitter and receiver. As a result, there is no signaling overload in the system that is affected by the use of the filters. In addition, the receiving filter helps in significantly increasing the signal-to-noise ratio (SNR) of the received F-OFDM signal to a maximum value [23]. Finally, the other receiver operations are performed in a reverse manner with respect to the transmitter.

5 | FILTER DESIGN

In F-OFDM, filter design plays an important role in the achievement of frequency localization of the signal and that of higher flexibility between the time and frequency localization. This is because the desired frequency-domain localization results in dispersion in the time domain [17]. In this section, we provide an example of a filter design that can significantly achieve a balanced time and frequency localization of the filter. In particular, the soft truncation of a prototype filter is employed using a time-domain window with smooth transitions. In the OFDM system, the signal displays a rectangular pulse shape (sinc function). This results in large side lobes for both the signal sides in the frequency domain. Accordingly, the frequency spectrum is not well-localized. A sinc impulse response filter, that is, a low-pass filter (LPF), is a suitable spectrum shaping filter for the F-OFDM system because of its capability to suppress OOBE. It does not distort the passband of the signal. Moreover, a time windowing mask is applied to provide good time localization and to ensure the smooth transitions for both ends of the filter impulse response in the time domain [16]. The FIR filter (windowing-sinc filter) is obtained by multiplying the sinc function and rooted raised cosine (RRC) that functions as a finite time-domain window. Therefore, the filter bandwidth can be defined as the total frequency width of the allocated subcarriers. In addition, a reasonable time localization is provided by the windowing in the truncated filter response. Because of the larger filter bandwidth of both Tx and Rx compared to that of the subcarrier spacing, the main energy time span of the time-domain end-to-end filter is notably smaller than the symbol length of OFDM. Furthermore, it is significantly smaller than the CP length when the tail is the filter's side lobe and the head of the filter does not cause overhead [25]. Therefore, the time-domain sinc impulse response filter can be expressed as

$$f(n) = h_{\mathrm{LPF}}(n) * w(n), \tag{9}$$

where

$$h_{\mathrm{LPF}}(n) = \frac{\sin(w_c * n)}{w_c * n}, \tag{10}$$

where $h_{\mathrm{LPF}}(n)$ is the low-pass filter sinc impulse response, w_c is the cutoff frequency of LPF, and $w(n)$ denotes the impulse response of windowing. In addition, the adoption of a suitable window function can achieve a flexible trade-off between the frequency and time localization. Hence, the ISI can be limited to an acceptable level. The RRC window function appears suitable for F-OFDM because it is more flexible than other windows such as Remez and Hanning [25]. Therefore, the time response of the RRC window is formulated as [33]

$$w_{\mathrm{RRC}}(n) = \left[0.5\ 1 + \cos\ \frac{2\pi n}{L-1}\ \right]^{\alpha}, \tag{11}$$

where α is the roll-off factor. It is the parameter that controls the window shape, and $0 < \alpha < 1$. The F-OFDM filter length is permitted to exceed the CP length to achieve higher flexibility for the filter design and to accomplish a significant balance between the time and frequency localization [34]. Hence, the filter length provides flexibility for the filter design. Here, the transition sharpness, passband flatness, and attenuation of the stopband are the major criteria to be satisfied by the filter for F-OFDM. In contrast, the large filter order value increases the complexity. Therefore, it should maintain the filter length above a certain limit. Meanwhile, the roll-off factor of the RRC window provides additional freedom for a significant balance between time and frequency localization. However, the window should have smooth transitions on both its sides to prevent abrupt upsurges at the start and end of the truncated filter. Therefore, it avoids the spillover frequency in the truncated filter. Thus, the roll-off factor is a parameter for controlling the window shape, and it provides additional freedom for the time and frequency localization balance. Therefore, the RRC window is more suitable for the F-OFDM system than other windows.

6 | SYSTEM EVALUATION

In this section, the OFDM and F-OFDM waveforms with and without PTS techniques are compared in terms of the PAPR

performance, frequency localization, BER, and processing complexity. The parameters of the simulation frame are determined as follows: N is 256 and 512, U is 4, M is fixed to 4, and the number of phase factors $R = 4$. Furthermore, an LPF and RRC windowing mask with a roll-off factor of 0.6 is employed for F-OFDM. The CCDF function is utilized to evaluate the PAPR for 1000 subframes of OFDM and F-OFDM. Meanwhile, 64-QAM and 16-PSK are adopted as a constellation mapping.

6.1 | PAPR performance

In this subsection, the PAPR performance of the OFDM and F-OFDM is evaluated based on the PTS technique. The simulation is performed for two values of N: 256 and 512. As is evident in Figure 3, when N is 256 and the CCDF probability is 10^{-3}, the PAPR of the F-OFDM waveform is higher than that of the standard OFDM by 1.66 dB. Meanwhile, the difference in PAPR performance between the two frameworks based on the PTS technique is 1.71 dB. Here, the PAPRs of PTS-OFDM and PTS-F-OFDM are 7.58 dB and 9.3 dB, respectively.

Similarly, Figure 4 depicts the PAPR performance of the OFDM and F-OFDM waveforms when $N = 512$. Compared to OFDM, F-OFDM increases the PAPR by 1.42 dB without PTS and by 1.73 dB with PTS. Accordingly, the results reveal that the PAPR of the F-OFDM waveform is higher than that of the OFDM standard by approximately 1.5 dB. This is because the filter length of the F-OFDM waveform causes the mean power of the signal to be lower than that of the OFDM standard. This results in an increase in the gap between the peak amplitude and mean value of the OFDM signal. Thereby, the PAPR performance is degraded. Meanwhile, the use of the PTS technique reduces the correlation among the samples within the subblocks and alters the phases of the samples. Hence, the peak amplitude of the signal is reduced.

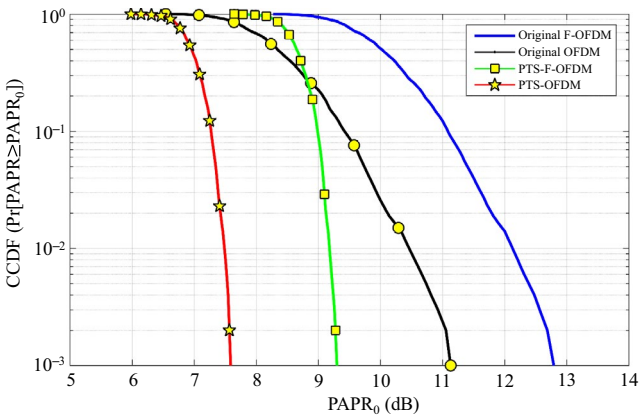

FIGURE 3 Comparison of PAPRs of OFDM and F-OFDM, $N = 256$

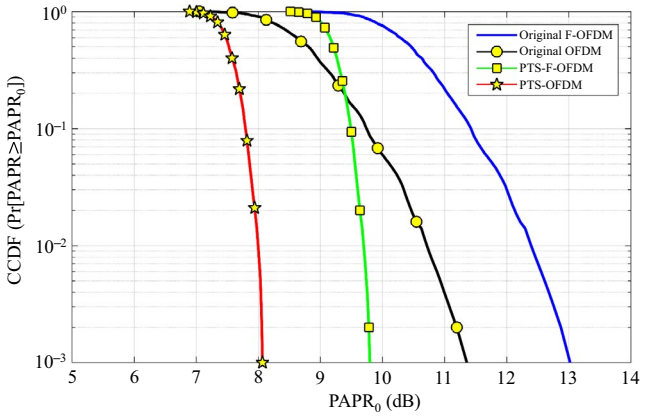

FIGURE 4 Comparison of PAPRs of OFDM and F-OFDM, $N = 512$

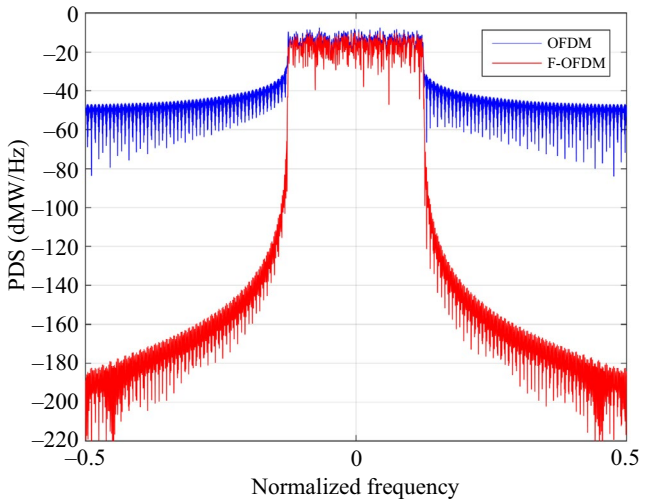

FIGURE 5 PSDs of OFDM and F-OFDM waveforms

This enhances the PAPR performance. Thus, the analysis and simulation indicate that the F-OFDM candidate waveform displays a high PAPR, which results in the degradation of the power amplifier efficiency at the transmitter. Nevertheless, we can employ the PAPR reduction techniques such as PTS, which can reduce the PAPR by over 3 dB from that of the original system.

6.2 | OOBE suppression

A significant advantage of filtering-based waveforms is the improvement in the spectral efficiency to satisfy the requirements of asynchronous transmission in 5G. The frequency localization of the OFDM and F-OFDM waveforms with and without PTS is evaluated by comparing the PSDs of both the waveforms. In the case of the F-OFDM waveform, the filter is designed with the filter length $L = 513$

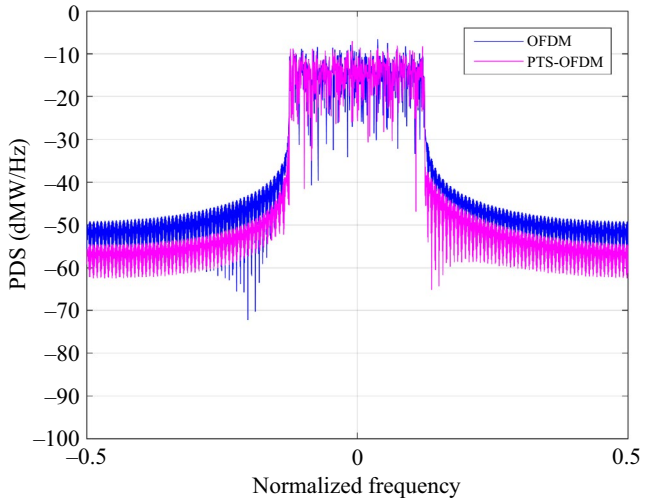

FIGURE 6 Comparison of PSDs of OFDM and PTS-OFDM

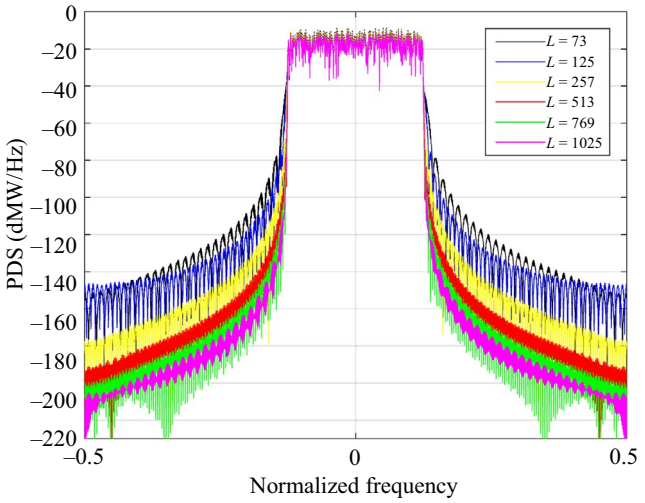

FIGURE 8 Comparison of PSD of F-OFDM with various filter lengths (L), when $\alpha = 0.6$

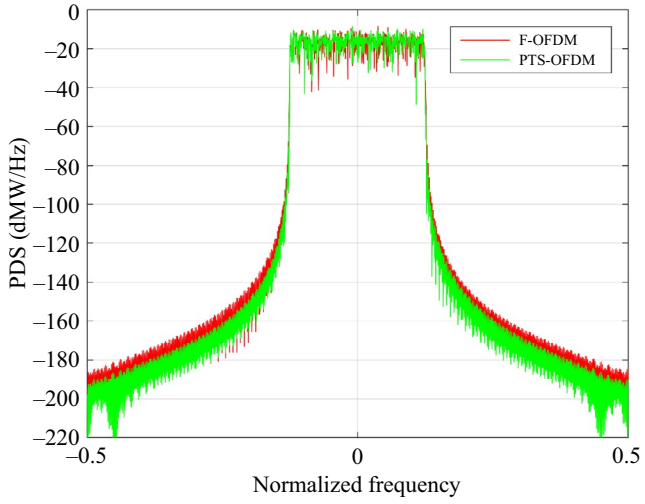

FIGURE 7 PSDs of F-OFDM and PTS-F-OFDM waveforms

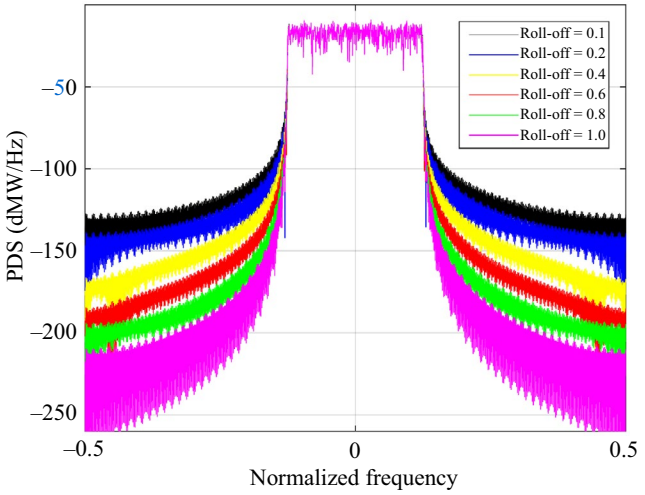

FIGURE 9 Comparison of PSD of F-OFDM with various roll-off factors (α) when $L = 513$

and roll-off factor $\alpha = 0.6$. Figure 5 presents the PSD of the OFDM and F-OFDM waveforms. Here, the OOBE power of the OFDM stander is –47 dB and that of the F-OFDM waveform is –185 dB. The results reveal that F-OFDM outperforms OFDM by reducing the OOBE by approximately 138 dB. Thus, the F-OFDM waveform has a higher level of frequency localization. This can be exploited to efficiently reuse spectrum in 5G.

Furthermore, the OFDM and F-OFDM waveform-based PTSs are illustrated in Figures 6 and 7, respectively. Here, the OOBE power of both the waveforms is reduced by less than 10 dB because the PTS technique improves the PAPR reduction performance. This results in a higher level of frequency localization and lower level of OOBE.

In addition, it is necessary to analyze the parameters that influence the OOBE power in the F-OFDM waveform framework. These parameters include the filter length, roll-off factor, and IFFT size. Figure 8 illustrates the power spectral density of the F-OFDM waveform with various filter lengths. It is evident that a longer filter produces a good frequency localization level and reduces the OOBE power. However, this improvement would be at the expense of increased computational complexity caused by the filter length. The filter length provides flexibility for the filter design. That is, a suitable filter length provides higher frequency localization and achieves effective filtering performance with regard to parameters such as passband flatness, sharpness of the transition band, and attenuation in the stop band. These are the main criteria to be satisfied by the filter for F-OFDM. In contrast, the large filter order value increases the complexity. Therefore, it should maintain the filter length above a certain limit. In this study, a filter length of up to half of the OFDM symbol length is selected

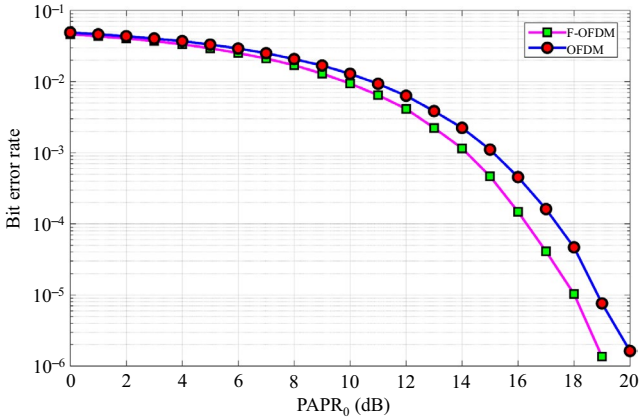

FIGURE 10 Comparison between 64-QAM BER of OFDM and F-OFDM for $N = 512$

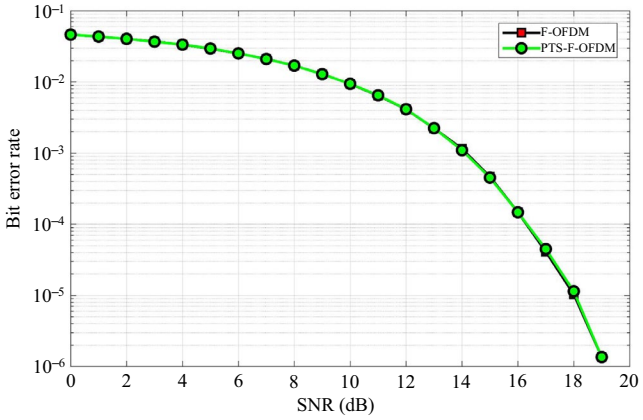

FIGURE 11 Comparison between 64-QAM BER of F-OFDM and PTS-F-OFDM for $N = 512$

to provide flexibility to filter design and to ensure ultimate filtering performance, so that there are no guard subcarriers between neighboring symbols.

Moreover, Figure 8 illustrates a PSD comparison for various filter lengths from $L = 73$ (equivalent to the number of cyclic prefixes) to $L = 1024$ (equivalent to the OFDM length). Meanwhile, the roll-off factor has been limited to 0.6. It is evident that the extended filter order improves the PSD performance. However, this would be at the expense of degraded complexity and ISI performances.

In addition, the roll-off factor can control the transition region for the window and provide a better balance between frequency and time localization. Figure 9 provides an example of the impact of the roll-off factor on OOBE when a filter length of half of the OFDM symbol length ($L = 513$) is selected. It is evident that an increase in the roll-off factor improves the OOBE suppression performance, considering that $\alpha = 1$ is a Hanning window, and $\alpha = 0$ is a rectangular window. Moreover, the IFFT size plays a vital role in frequency localization, where the large IFFT size provides more density and details, which are effective graphically. Furthermore, it ensures a symmetrical spectrum representation of the signal and spreads the spectrum on the symbols uniformly [35]. Accordingly, the analysis and simulation indicate that the F-OFDM waveform outperforms the OFDM standard with respect to OOBE suppression. This results in a more efficient reuse of the spectrum to support the non-synchronous transmission and reduce the latency of 5G.

6.3 | BER performance

In this subsection, the evaluation of the BER performance of the OFDM and F-OFDM waveforms is presented. The BER performance is simulated using the Monte Carlo procedure. Figures 10, 11, and 12 present curves that represent the relationship between the BER of the OFDM system and that of the F-OFDM waveform. In Figures 10 and 11, the AWGN channel is adopted, constellation mapping of both the frameworks is set to 64-QAM, and number of subcarriers is fixed to 512. It is evident that the BER of F-OFDM is almost similar to that of OFDM at low values of SNR. Meanwhile, the BER performance of F-OFDM is partly higher than that of OFDM at large values of SNR. It is evident from Figure 10 that the BER probability of the F-OFDM system is 9.3×10^{-3}, 4.6×10^{-4}, and 4.1×10^{-5} at the SNR values of 10, 15, and 17, respectively. Meanwhile, the BER probability of the OFDM system is 1.2×10^{-2}, 1.1×10^{-3}, and 1.6×10^{-4} at the same values of SNR. The BER performance of the F-OFDM with and without PTS technique has been simulated in Figure 11. In this case, the BER performance of both the signals is identical because of the probabilistic nature of the PTS technique. In Figure 12, the BER performance for both the systems has been evaluated based on a multipath fading channel (Rayleigh channel). It is evident that the BER performance of the F-OFDM system is higher than that of the OFDM systems for both the channels. This is because the windowing provides a reasonable time localization in the truncated filter's response, which causes the ISI of the F-OFDM signal to be maintained within an acceptable limit and also better than that of the OFDM system.

Meanwhile, Figure 13 presents the BER performance of OFDM and F-OFDM while using 16-PSK constellation mapping. Here, the BER probability of F-OFDM when $N = 256$ is 1.5×10^{-2} and 1.17×10^{-4} at the SNR values of 7 and 14, respectively. However, the BER of the OFDM system is 2.5×10^{-2} and 6.5×10^{-4} at the SNR values of 7 and 14, respectively. Moreover, Figure 14 shows the BER performance of F-OFDM with and without PTS. The two curves are identical. In addition, Figure 15 presents the BER performance of both the systems when the Rayleigh channel is used. Hence, the F-OFDM system outperforms the OFDM system for both channels.

It is evident from the results obtained that the PSK constellation mapping improves the BER performance of both

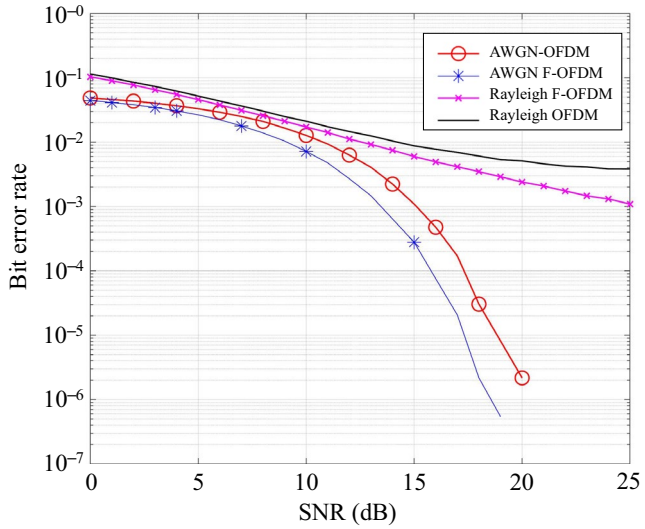

FIGURE 12 Comparison between 64-QAM BER of F-OFDM and OFDM for $N = 512$, AWGN, and Rayleigh channels

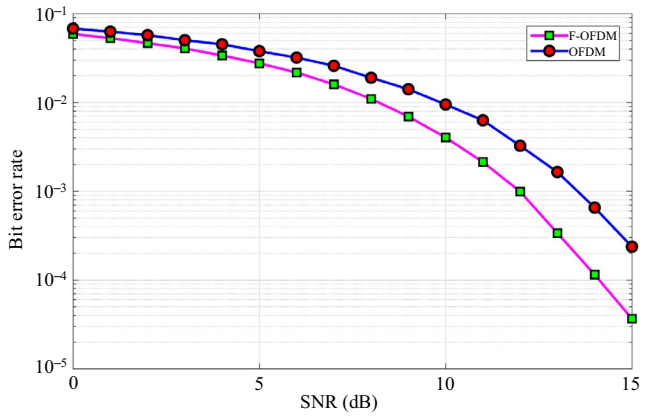

FIGURE 13 Comparison between 16-PSK BER of F-OFDM and F-OFDM for $N = 256$

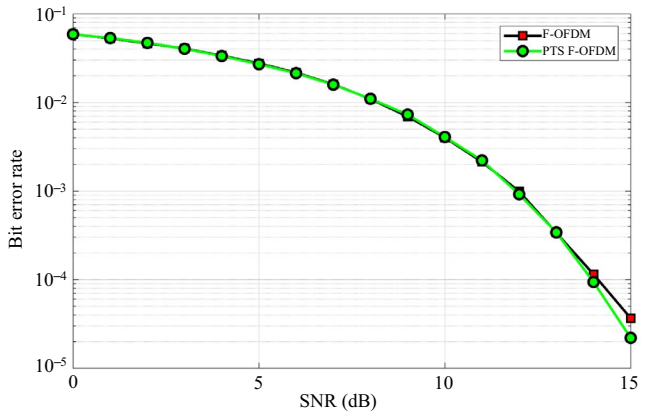

FIGURE 14 Comparison between 16-PSK BER of F-OFDM and PTS-F-OFDM for $N = 256$

the systems compared with that of the 64-QAM modulation family. Furthermore, the F-OFDM waveform still has priority over OFDM at medium and large values of SNR. In addition,

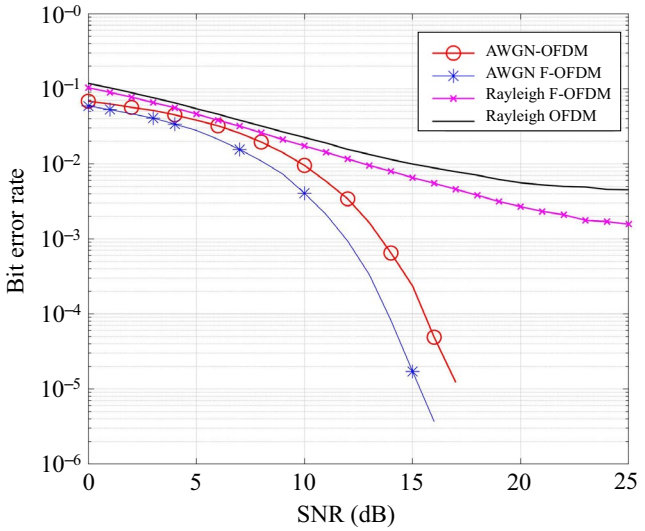

FIGURE 15 Comparison between 16-PSK BER of F-OFDM and OFDM for $N = 256$, AWGN, and Rayleigh channels

TABLE 1 Computational complexity of PTS-OFDM and PTS-F-OFDM ($M = 4$, $R = 4$)

	Computational complexity of PTS-OFDM		Computational complexity of PTS-F-OFDM	
N	CC^{add}_{OFDM}	CC^{mult}_{OFDM}	CC^{add}_{F-OFDM}	CC^{mult}_{F-OFDM}
256	57 344	86 016	57 344	217 344
	Increase in multiplication = 60.42%			
512	116 736	173 056	116 736	435 712
	Increase in multiplication = 60.28%			

the BER performance depends on the modulation family used and order of constellation mapping. Here, a high-order constellation increases BER degradation because it is more sensitive to the interference. Moreover, the improvement in the BER performance of the F-OFDM waveform is because of the filter window, which reduces the ISI between the adjacent symbols. Furthermore, the BER performances of PTS-OFDM and PTS-F-OFDM display results similar to those of OFDM and F-OFDM. This is because the PTS technique is a probabilistic method and did not cause signal distortion. Accordingly, the BER performance of the F-OFDM waveform is higher than that of the OFDM stander for all the values of SNR, and the BER performance remains uninfluenced by the use of the PTS technique.

6.4 | Computational complexity

The computational complexity of the PTS-OFDM system can be classified into two parts: the IFFT calculations and the calculations for determining the optimum phase factor. Here, the

computational complexity level in the frequency domain (IFFT complexity) is the number of complex addition and multiplication operations within the IFFT unit for converting the data of subblocks from the frequency domain to the time domain. Meanwhile, an exhaustive search should be performed in the time domain to identify the optimum phase factor. This is because R^{M-1} phase factor vectors are examined. Here, R is the number of permitted phase factors. Moreover, the first element of the set of phase factors is generally fixed to one without performance loss. In addition, the phase rotation factors must have an amplitude of unity, and they generally are limited to $\{\pm 1\}$ or $\{\pm 1, \pm j\}$ to avoid the additional complex multiplication operations. Therefore, the number of addition operations $\mathrm{CC}^{\mathrm{add}}_{\mathrm{OFDM}}$ and multiplication operations $\mathrm{CC}^{\mathrm{mult}}_{\mathrm{OFDM}}$ of the OFDM system can be expressed as the formulas presented below [36]. The oversampling factor and the complexity of the comparison operations for selecting the best OFDM signal are omitted.

$$\mathrm{CC}^{\mathrm{add}}_{\mathrm{OFDM}} = MN\log_2 N + R^{M-1}N(M-1) \tag{12}$$

and

$$\mathrm{CC}^{\mathrm{mult}}_{\mathrm{OFDM}} = \frac{MN}{2}\log_2 N + R^{M-1}N(M+1). \tag{13}$$

Meanwhile, the computational complexity of the PTS-F-OFDM waveform in the transmitter includes the IFFT complexity, phase factor complexity, and filter complexity. Here, the added filter increases the number of complex multiplication operations in the PTS-F-OFDM system. This complexity depends on the filter length. Hence, the number of complex multiplications operations in the PTS-F-OFDM system represents the number of multiplication operations in the OFDM system and the number of operations in multiplying the filter length (L) by the OFDM length (N). Therefore, $\mathrm{CC}^{\mathrm{add}}_{\mathrm{F-OFDM}}$ and $\mathrm{CC}^{\mathrm{mult}}_{\mathrm{F\text{-}OFDM}}$ can be formulated as [37,38]:

$$\mathrm{CC}^{\mathrm{add}}_{\mathrm{F-OFDM}} = MN\log_2 N + R^{M-1}N(M-1) \tag{14}$$

and

$$\mathrm{CC}^{\mathrm{mult}}_{\mathrm{F-OFDM}} = \frac{MN}{2}\log_2 N + R^{M-1}N(M+1) + N(L-1). \tag{15}$$

Table 1 documents the computational burden of OFDM and F-OFDM based on the PTS technique. Here, M and R are set to 4, and the filter length $L = 513$. When the number of subcarriers is 256, the computational complexity of PTS-OFDM is $\mathrm{CC}^{\mathrm{add}}_{\mathrm{OFDM}} = 57\ 344$ and $\mathrm{CC}^{\mathrm{mult}}_{\mathrm{OFDM}} = 86\ 016$. Meanwhile, $\mathrm{CC}^{\mathrm{add}}_{\mathrm{F-OFDM}}$ and $\mathrm{CC}^{\mathrm{mult}}_{\mathrm{F-OFDM}}$ of PTS-F-OFDM are 57 344 and 217 344, respectively. In addition, when $N = 512$, the addition operations of PTS-OFDM and PTS-F-OFDM are 116 736. In addition, the number of multiplication operations of PTS-OFDM and PTS-F-OFDM is 173 056 and 435 712, respectively. It is evident that the number of multiplication operations of the F-OFDM system is higher than that of the OFDM system by 60%. This is because of the additional complexity resulting from the application of the filter. Therefore, the computational complexity level of F-OFDM with respect to that of OFDM is associated with the filter length: An increase in the filter length results in an increase in the computational complexity level and vice versa.

7 | CONCLUSION

The essential objective of the paper is to highlight the PAPR performance of the F-OFDM waveform framework, which is being considered as a candidate for 5G. The PAPR performance of F-OFDM based on the PTS technique is evaluated and compared with PTS-OFDM. We have addressed the PAPR performance as well as the other related parameters such as OOBE suppression, BER, and computational complexity. An important implication of the simulation results is that the PTS technique causes a reduction in the PAPR of F-OFDM by over 3 dB, suppression of OOBE by approximately 10 dB, and un-influencing of the BER performance. In contrast, the main limitation of the application of the PTS technique to F-OFDM is the increase in the computational complexity of the system owing to the added filter. Therefore, the F-OFDM framework based on the PTS technique is an effective waveform design for 5G with regard to the PAPR reduction performance and OOBE suppression, considering the balance between the computational complexity and performance. In our future research, we intend to concentrate on the reduction in the computational complexity of PTS-F-OFDM without degradation in performance.

ORCID

Yasir Amer Al-Jawhar https://orcid.org/0000-0002-6506-5433

REFERENCES

1. P. P. Kumar and K. K. Kishore, *BER and PAPR analysis of UFMC for 5G communications*, Indian J. Sci. Technol. **9** (2016), 1–6.
2. Q. Bodinier, F. Bader, and J. Palicot, *Coexistence of filter banks and CP-OFDM: What are the real gains?*, in Proc. Int. Symp. Wireless Commun. Syst. (Poznan, Poland), Sept. 2016, pp. 628–632.
3. G. Wunder et al., *5GNOW: Non-orthogonal, asynchronous waveforms for future mobile applications*, IEEE Commun. Mag. **52** (2015), 97–105.
4. J. Li et al., *Cognitive radio network assisted by OFDM with index modulation*, IEEE Trans. Veh. Technol. **69** (2020), 1106–1110.
5. J. Li et al., *Layered orthogonal frequency division multiplexing with index modulation*, IEEE Syst. J. **13** (2019), 3793–3803.

6. Y. A. Jawhar et al., *A low PAPR performance with new segmentation schemes of partial transmit sequence for OFDM systems*, Int. J. Adv. Appl. Sci. **4** (2017), 14–21.
7. N. Taspinar and Y. T. Bozkurt, *PAPR reduction using genetic algorithm in lifting-based wavelet packet modulation systems*, Turk. J. Electr. Eng. Comp. Sci. **24** (2016), 184–195.
8. L. Zhang et al., *Filtered OFDM systems, algorithms and performance analysis for 5G and beyond*, IEEE Trans. Commun. **66** (2017), 1–14.
9. F. Schaich, T. Wild, and Y. Chen, *Waveform contenders for 5G-suitability for short packet and low latency transmissions*, in Proc. IEEE Conf. Veh. Technol. Conf. (Seoul, Rep. of Korea), May 2014, pp. 1–5.
10. X. Wang, K. Kienzle, and S. T. Brink, *On spectral shaping of multicarrier waveforms employing FIR-filtering and active interference cancellation*, in Proc. Int. ITG Conf. Syst. Commun. Coding (Hamburg, Germany), Feb. 2017, pp. 1–6.
11. Y. Liu et al., *Waveform design for 5g networks: Analysis and comparison*, IEEE Access **5** (2017), 19282–19292.
12. S. Tabatabaee and H. Zamiri-Jafarian, *Prototype filter design for FBMC systems via evolutionary PSO algorithm in highly doubly dispersive channels*, Trans. Emerg. Telecommun. Technol. **28** (2017), article no. e3048.
13. X. Wang, T. Wild, and F. Schaich, *Filter optimization for carrier-frequency-and timing-offset in universal filtered multi-carrier systems*, in Proc. IEEE Veh. Technol. Conf. (Glasgow, UK), May 2015, pp. 1–6.
14. L. Zhang et al., *Subband filtered multi-carrier systems for multi-service wireless communications*, IEEE Trans. Wireless Commun. **16** (2017), 1893–1907.
15. P. Weitkemper et al., *On regular resource grid for filtered OFDM*, IEEE Commun. Lett. **20** (2016), 2486–2489.
16. J. Wang et al., *Spectral efficiency improvement with 5G technologies: Results from field tests*, IEEE J. Sel. Area. Commun. **35** (2017), 1867–1875.
17. R. Gerzaguet et al., *The 5G candidate waveform race: A comparison of complexity and performance*, EURASIP J. Wirel. Commun. Netw. **13** (2017), 1–14.
18. J. Li et al., *Generalized pre-coding aided quadrature spatial modulation*, IEEE Trans. Veh. Technol. **66** (2017), 1881–1886.
19. M. Singh and S. Patra, *Partial transmit sequence optimization using improved harmony search algorithm for PAPR reduction in OFDM*, ETRI J. **39** (2017), 782–793.
20. M. A. Taher et al., *Reducing the PAPR of OFDM systems by random variable transformation*, ETRI J. **35** (2013), 714–717.
21. Z. Wang, J. Zhu, and K. Gao, *Proposal of PAPR reduction method for OFDM signal by optimized PTS combined with interleaving method*, in Proc. IEEE China Summit Int. Conf. Signal Inf. Process. (Chengdu, China), July 2015, pp. 943–947.
22. J. Li, E. Bala, and R. Yang, *Resource block filtered-OFDM for future spectrally agile and power efficient systems*, Phys. Commun. **11** (2014), 36–55.
23. J. Abdoli, M. Jia, and J. Ma, *Filtered OFDM: A new waveform for future wireless systems*, in Proc. IEEE Int. Workshop Signal Process. Adv. Wireless Commun. (Stockholm, Sweden), 2015, pp. 66–70.
24. X. Zhang et al., *Filtered-OFDM-enabler for flexible waveform in the 5th generation cellular networks*, in Proc. IEEE Conf. Glob. Commun. Conf. (San Diego, CA, USA), Dec. 2015, pp. 1–6.
25. D. Wu et al., *A field trial of F-OFDM toward 5G*, in Proc. IEEE Globecom Workshop. (Washington, DC, USA), Dec. 2016, pp. 1–6.
26. P. Weitkemper et al., *Adaptive filtered OFDM with regular resource grid*, in Proc. IEEE Int. Conf. Commun. Workshop. (Kuala Lumpur, Malaysia), May 2016, pp. 462–467.
27. Y. Jawhar et al., *New low complexity segmentation scheme of partial transmit sequence technique to reduce the high PAPR value in OFDM systems*, ETRI J. **40** (2018), 1–15.
28. Y. Al-Jawhar et al., *A new subblock segmentation scheme in partial transmit sequence for reducing PAPR value of the OFDM systems*, Int. J. Integr. Eng. **10** (2018), 91–97.
29. C. Kang et al., *A low complexity PAPR reduction method based on FWFT and PEC for OFDM systems*, IEEE Trans. Broadcast. **63** (2017), 416–425.
30. Y. Al-Jawhar et al., *A new partitioning scheme for PTS technique to improve the PAPR performance in OFDM systems*, Int. J. Eng. Technol. Innov. **8** (2018), 217–227.
31. N. Taspinar and Y. T. Bozkurt, *Peak-to-average power ratio reduction using backtracking search optimization algorithm in OFDM systems*, Turk. J. Electr. Eng. Comp. Sci. **24** (2016), 2307–2316.
32. R. Salmanzadeh and B. Tazehkand, *A modified method based on the discrete sliding norm transform to reduce the PAPR in OFDM systems*, ETRI J. **36** (2014), 42–50.
33. P. Guan et al., *5G field trials: OFDM-based waveforms and mixed numerologies*, IEEE J. Sel. Area. Commun. **35** (2017), 1234–1243.
34. F. Schaich and T. Wild, *Waveform contenders for 5G—OFDM vs. FBMC vs. UFMC*, in Proc. Int. Symp. Commun, Contr. Signal Process. (Athens, Greece), May 2014, pp. 457–460.
35. Y. Al-Jawhar et al., *Zero-padding techniques in OFDM systems*, Int. J. Electr. Eng. Inform. **10** (2018), 704–725.
36. Y. Jawhar et al., *A review of partial transmit sequence for PAPR reduction in the OFDM systems*, IEEE Access **7** (2019), 18021–18041.
37. K. Tani et al., *PAPR reduction of post-OFDM waveforms contenders for 5G & Beyond using SLM and TR algorithms*, in Proc. IEEE Inter. Conf. Telecommun. (St. Malo, France), June 2018, pp. 104–109.
38. Y. Jawhar et al., *Reducing PAPR with low complexity for 4G and 5G waveform designs*, IEEE Access **7** (2019), 97673–97688.

AUTHOR BIOGRAPHIES

Yasir Amer Al-Jawhar received his BS degree in electrical engineering from the College of Engineering, University of AL-Mustansiriya, Baghdad, Iraq, in 1998, and his MS degree in engineering from the Faculty of Electrical and Electronic Engineering, University Tun Hussein Onn Malaysia, Johor, Malaysia, in 2015. He received his PhD in communication engineering from the University Tun Hussein Onn Malaysia in 2019. His main research interests are signal processing in communication, OFDM, PAPR reduction in Multicarrier system, 5G waveform design, and wireless network.

Khairun N. Ramli received his BS degree in electrical engineering from the University of Manchester Institute of Science and Technology, Manchester, United Kingdom, in 1997, his MS degree in engineering from the Universiti Kebangsaan Malaysia, Kula Lumpur, Malaysia, in 2004, and his PhD for research in electromagnetic analysis from the University of Bradford, United Kingdom, in 2011. Since 2011, he has been associated with the Faculty of Electrical and Electronic Engineering, University Tun Hussein Onn Malaysia, Johor, Malaysia, where he is a senior lecturer. His main research interests are wireless technologies, antennas, electromagnetics, and engineering computing.

Montadar Abas Taher received his BS degree in electronics and communications engineering from the Al-Nahrain University, Baghdad, Iraq, in 2000, his MS degree in satellite engineering from the Al-Nahrain University, Iraq, in 2003, and his PhD from the University Kebangsaan Malaysia, Kula Lumpur, Malaysia, in 2015. Since 2010, he has been associated with the Department of Communication, University of Diyala, Diyala, Iraq, where he is a senior lecturer. His main research interests are OFDM, CDMA, MC-CDMA, PAPR reduction in multicarrier systems, and DSP for telecommunication.

Nor Shahida M. Shah received her BS degree in electrical engineering from the Tokyo Institute of Technology, Tokyo, Japan, in 2000, her MS degree from the University of Malaya, Kula Lumpur, Malaysia, in 2003, and her PhD from Osaka University, Tokyo, Japan, in 2012. Since 2011, she has been associated with the Faculty of Electrical and Electronic Engineering, University Tun Hussein Onn Malaysia, Johor, Malaysia, where she is a senior lecturer. Her main research interests are optical fiber devices, optical communication, nonlinear optics, optical signal processing, antenna and propagation, and wireless communication.

Salama A. Mostafa is currently a postdoctoral staff at UTHM, Malaysia. He obtained his BSc degree in computer science from the University of Mosul, Iraq, in 2003. He obtained his MSc and PhD degrees in information technology from UNITEN, Malaysia, in 2011 and 2016, respectively. His research interests are soft computing, data mining, and intelligent autonomous systems.

Bashar Ahmed Khalaf received his BSc degree in computer science from Diyala University, Iraq, in 2011, and his MSc degree from the Computer Science Networks Department, Universiti Tun Hussein Onn Malaysia (UTHM), in 2019. His research interest in Network Security includes DDoS attack and defense approaches.